RAR: Real-Time Acoustic Ranging in Underwater Sensor Networks

Yonghun Kim, *Student Member, IEEE*, Youngtae Noh, *Member, IEEE*, and Kiseon Kim, *Senior Member, IEEE*

***Abstract*— As a core component of underwater localization, accurate acoustic ranging is quite challenging because of the harsh characteristics of underwater environments (e.g., refraction and reflection). To enhance ranging accuracy, ranging schemes employing a ray tracing model and a sound speed profile have been proposed; however, the existing schemes require numerous ray tracing iterations to perform ranging estimation within a certain range of accuracy. This renders the solutions that they generate impractical for real-time localization. In this letter, we propose a novel ranging scheme called real-time acoustic ranging (RAR). To reduce computational overhead while maintaining reliable accuracy, RAR exploits the property of ray pattern locality, whereby spatially proximate rays exhibit similar patterns. The results revealed that RAR can ensure a better tradeoff between accuracy and computational overhead than a state-of-the-art solution.**

***Index Terms*— Acoustic ranging, localization, underwater sensor networks, ray tracing, real-time.**

I. Introduction

RECENT research interest in underwater acoustic sensor networks (UASNs) suggests that such networks are effective tools for exploring and understanding bodies of water for such fields as marine environment monitoring, disaster prevention, and the gathering of oceanographic data for scientific purposes [1]. In these areas, identifying the locations of sensor nodes plays an important role in the spatio-temporal tagging of the collected oceanographic data.

Intensive work has been reported in the literature on underwater localization to deliver accurate location services [2]. However, only a handful of studies on underwater ranging, a building block of range-based localization, have been conducted. While ranging simply measures the distance between nodes, achieving high accuracy therein is a challenging problem because of the harsh environmental characteristics of the acoustic underwater medium (*i.e.,* refraction, reflection, and multipath fading) [1]. Most ranging schemes proposed in previous studies on the subject are vulnerable to the effect of variations in the speed of sound ([3] and [4] are exceptions).

Manuscript received May 18, 2017; revised July 5, 2017; accepted July 27, 2017. Date of publication August 11, 2017; date of current version November 9, 2017. We gratefully acknowledge that the SAVEX15 data was provided by KRISO (No. PES1940), by KIOST (No. PES99331), and by MPL and ONR (No. N00014-31-1-0510). This research was a part of the project titled 'Development of Ocean Acoustic Echo Sounder and Hydro-Physical Properties Monitoring Systems', funded by the ministry of Oceans and Fisheries, Korea, and also supported in part by Basic Science Research Program through the National Research Foundation of Korea (NRF) funded by the Ministry of Education (No. NRF-2016R1C1B2011415), Inha University Research Grant (No. 54465-01). The associate editor coordinating the review of this letter and approving it for publication was M. Erol-Kantarci. *(Corresponding authors: Kiseon Kim; Youngtae Noh.)*

Y. Kim and K. Kim are with the School of Electrical Engineering and Computer Science, Gwangju Institute of Science and Technology, Gwangju 61005, South Korea (e-mail: mizpah@gist.ac.kr; kskim@gist.ac.kr).

Y. Noh is with the Department of Computer Engineering, Inha University, Incheon 22212, South Korea (e-mail: ytnoh@inha.ac.kr).

Digital Object Identifier 10.1109/LCOMM.2017.2738628

In [3], Ameer and Jacob proposed a ray bending-based localization (RBL) scheme to find the locations of sensor nodes with a known depth-dependent sound speed profile (SSP). This scheme considered only the ray bending phenomenon (*i.e.,* refraction) but not reflection, and hence only partially improved localization accuracy [3]. Most recently, Ramezani *et al.* proposed a ray-based root finding ranging (RRFR) scheme [4]. Compared to RBL, RRFR considered not only direct paths with refraction but also various acoustic ray patterns under refraction and reflection. Moreover, the scheme used pressure sensors to accurately measure the depths of the sensor nodes. Given the depths of two nodes and the time of arrival (ToA), the scheme calculated the horizontal distance through a root finding algorithm. The authors reported that the RRFR scheme outperformed prevalent schemes.

However, as the root finding algorithm of RRFR relies on "plane binary search" to estimate the locations of sensor nodes, it requires numerous ray tracing iterations; as a result, RRFR incurs high computational cost and considerable waiting time. We note that a single ray tracing iteration expends a considerable amount of computation time according to the specifications of the hardware, the simulation parameters, and the distance between nodes [5]; hence, RRFR may not be suitable for real-time applications, such as localization and tracking, which require more computational ranging processes according to the number of beacon and sensor nodes [6]. Motivated by this, in this letter, we propose Real-time Acoustic Ranging (RAR), a novel ranging scheme based on a ray tracing model. Given the ToA, RAR exploits the observation that spatially proximate rays exhibit similar patterns. The phenomenon is called *ray pattern locality*, and is easily observed in such ray tracing models as Bellhop as well as in practice. By harnessing this property, RAR reduces the search space for distance estimation between points with high accuracy, thus significantly reducing the number of ray tracing iterations and their computational overhead in RRFR, and in turn making it possible to support real-time applications. This letter makes the following contributions:

- We propose RAR, a novel real-time ranging scheme. RAR harnesses ray pattern locality to provide accurate distance estimation in real time.
- To evaluate RAR's performance with respect to accuracy and computational overhead matrices, we present the results of simulations and experiments conducted near Jeju Island in Korea. The results verified that RAR attained an accuracy very close to that of RRFR and was at least six times faster.

II. RAR Algorithm

In this section, we first describe a ranging estimation problem with reasonable assumptions for approximation. We then present the procedure of the RAR scheme.

A. Problem Description and Assumptions

We consider ranging estimation based on the measured ToA of a single acoustic transmission between a source and a receiver. Given the measured ToA value between nodes to compute their distance, we adopt Bellhop, a representative ray tracing model to consider more realistic acoustic ray propagation [5]. The Bellhop model can compute acoustic fields via Gaussian beam tracing and predict the ray trajectories of arrivals using certain required parameters as inputs, such as the horizontal distance (d) between nodes, SSP in the direction of depth z ($c(z)$), bathymetric information (B), the depths of the source (z_s) and the receiver (z_r), signal frequency (f_s), and the number of launched rays (N_{ray}) between angles.

For estimation, we assume that the receiver can identify the fastest ray among the arrivals to obtain its elapsed time as ToA and measure its depth z_r through a pressure sensor. Moreover, we exploit the observation that ray arrivals exhibit similar patterns in spatial proximity, *i.e., ray pattern locality*, which is easily observed in real life as well as in a Bellhop simulation. More precisely, there are similar ray patterns between the actual range and the estimated proximal range unless the latter is not far from the former. This phenomenon has been widely reported in oceanographic literature [7]. By harnessing this characteristic, the computational complexity of conventional schemes based on a plain binary search can be remarkably reduced.

Let's define d and l representing the horizontal straight-line distance from the source and the total length of the trajectory, respectively. Given ToA t_m, we can initially estimate the length of the trajectory r_{traj}, denoted by $\hat{l}_{initial}$, between nodes with the following simple equation:

$$\hat{l}_{initial} = \hat{c} \times t_m, \tag{1}$$

where $\hat{c}$ is a nominal constant of the maximum sound speed from the given SSP and t_m is the elapsed time of the selected fastest ray. We here use the stretched length of $\hat{l}_{initial}$ as a horizontal distance value, denoted by $\hat{d}_{1st}$. Although $\hat{d}_{1st}$ can be given as an initially estimated range, it considers only the presumably nominal value of the given SSP, and hence only provides a coarse estimation of the actual range d. Furthermore, it introduces a considerable error because it ignores the effects of variations in the speed of sound and the trajectories of the acoustic rays. Thus, the equation can be altered as follows:

$$\hat{d}_{1st} = d + \epsilon_{ss} + \epsilon_{traj}, \tag{2}$$

where ϵ_{ss} is the biased displacement from the given location caused by unknown signal speed variations, and ϵ_{traj} is the biased displacement from the given location caused by unknown acoustic ray trajectories. Our objective is to estimate the actual range d by compensating for the overall bias-induced errors ($\epsilon_{ss} + \epsilon_{traj}$).

B. Procedure of the Proposed Algorithm

1) Sound Speed Compensation: Because a nominal constant sound speed $\hat{c}$ cannot account for the actual trajectory of a ray, error ϵ_{ss} is introduced due to the use of an incorrect sound speed value. As shown in Fig. 1(a), the first part of Algorithm 1, sound speed compensation, is used to reduce error ϵ_{ss}.

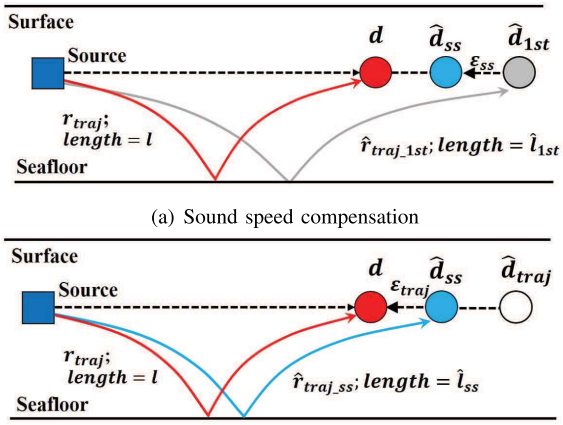

(a) Sound speed compensation

(b) Ray trajectory compensation

Fig. 1. Schematic diagram of the RAR algorithm.

Algorithm 1 RAR Algorithm

Input: Measured ToA t_m, $c(z)$, B, z_s, z_r, f_s, N_{ray}
Output: $\hat{d}_{RAR}$
Initialization
  $\hat{l}_{initial} = \hat{c} \times t_m$, where $\hat{c} = max_z c(z)$
  $\hat{d}_{1st} \leftarrow \hat{l}_{initial}$
Procedure: Sound speed compensation
Compute actual length of the fastest ray $\hat{l}_{1st}$ corresponding to minimum ToA $\hat{t}_{1st}$ at $\hat{d}_{1st}$.
  $\hat{t}_{1st}, \hat{l}_{1st} \leftarrow$ BELLHOP $(\hat{d}_{1st}, c(z), B, z_s, z_r, f_s, N_{ray})$
Compute the estimated range $\hat{d}_{ss}$ with corrected speed $\hat{c}_{ss}$.
  $\hat{c}_{ss} = \hat{l}_{1st}/\hat{t}_{1st}$
  $\hat{l} = \hat{c}_{ss} \times t_m$
  $\hat{d}_{ss} \leftarrow \hat{l}$
End procedure
Procedure: Trajectory compensation
Compute actual length of the fastest ray $\hat{l}_{ss}$ at $\hat{d}_{ss}$, and its horizontal distance value d_{traj}
  $\hat{l}_{ss} \leftarrow$ BELLHOP$(\hat{d}_{ss}, c(z), B, z_s, z_r, f_s, N_{ray})$
  $\hat{d}_{traj} \leftarrow \hat{l}_{ss}$
Compute the final estimated range $\hat{d}_{RAR}$.
  $\hat{d}_{RAR} = 2 \cdot \hat{d}_{ss} - \hat{d}_{traj}$
End procedure

It is necessary to reset the mean speed of the ray-based sound as $\hat{c}_{ss}$ by predicting the pattern of the actual ray. To obtain $\hat{c}_{ss}$, we run a round of the Bellhop simulation and identify the fastest ray arriving at constant sound speed $\hat{c}$ at $\hat{d}_{1st}$. Through the Bellhop simulation, we can easily compute the total length $\hat{l}_{1st}$ traveled along $\hat{r}_{traj\_1st}$ and its elapsed time as $\hat{t}_{1st}$. $\hat{c}_{ss}$ can in turn be computed as $\hat{l}_{1st}/\hat{t}_{1st}$. The compensated length $\hat{l}$ can then be computed as follows:

$$\hat{l} = \hat{c}_{ss} \times t_m. \tag{3}$$

2) Trajectory Compensation: Besides sound speed compensation for ϵ_{ss}, another bias error, denoted by ϵ_{traj}, is introduced due to the effect of refraction and reflection, as shown

in Fig. 1(b). To remove the bias error ϵ_{traj}, the second part of Algorithm 1, trajectory compensation, is used. To reduce the number of iterations of ray tracing, we use two key approximations according to *ray pattern locality*. The first is that the actual length l can be updated as $\hat{l}$, and we here use the stretched length of $\hat{l}$ as the distance value, denoted by $\hat{d}_{ss}$. This is because $\hat{c}_{ss}$ is very close to the actual sound speed c_{real} of d through the ray pattern prediction of the previous step. The second key approximation to reduce the number of iterations of ray tracing is that the trajectory error ϵ_{traj} at d can be approximated as the difference between $\hat{d}_{ss}$ and the horizontal distance of the length $\hat{l}_{ss}$, denoted by $\hat{d}_{traj}$. This is because ϵ_{traj} is biased by the effects of both refraction and reflection, and $\hat{d}_{traj}$ also contains a similar bias error due to refraction and reflection under similar patterns. Therefore, the same locality applies here, and we can calculate the final estimated range $\hat{d}_{RAR}$ as follows:

$$\hat{d}_{RAR} = 2 \cdot \hat{d}_{ss} - \hat{d}_{traj}. \tag{4}$$

III. Simulations

In this section, we evaluate the performance of RAR in comparison with RRFR with respect to accuracy and computational overhead. We first describe our simulation scenario and the configured parameters.

For the simulations, we first deployed a source and a receiver at a depth of 40 m and varied the distance between them from 500 m to 6,000 m. We used a measured SSP in a shallow water area near Jeju Island (on May 21, 2015, as shown in Fig. 3). The depth of the flat seafloor (from sea surface) was 100 m. We used a Bellhop model assisted by the Actoolbox in MATLAB [5]. For every measurement, we generated 300 rays with a signal frequency of 10kHz.

To evaluate the accuracies of both the RAR and the RRFR schemes, we considered the distance-dependent range measurement error model (as in [3]) and the depth measurement error model with Gaussian distributions $N(0, {\sigma_r}^2)$ and $N(0, {\sigma_{z_r}}^2)$, where the standard deviation of the measured range σ_r was $0.001 \times d$ m (*i.e.,* 0.1% of actual distance d) and that of the measured depth σ_{z_r} was 1 m. We set distances varying from 500 m to 6,000 m with gaps of 500 m and measured the ToAs at each location. We then calculated the accuracy of both schemes in terms of normalized range errors (NRE) with respect to actual distance d between source and receiver (*i.e.,* $NRE(\%) = \frac{\hat{d}-d}{d} \times 100$). Note that the NRE can be positive or negative (*i.e.,* overestimation or underestimation) due to its definition as in [8]. To evaluate the computational overhead of the schemes, we measured their accuracies and the run times on an off-the-shelf workstation (Intel Core i7-4700MQ, 2.40GHz with 8.0GB RAM).

Figure 2 shows the NRE of both schemes by averaging over 200 simulations with a confidence interval of 95%. In the figure, the uppermost solid black line shows the initial estimation error with a presumably constant sound speed. The main errors in the initial estimation error were ϵ_{ss}, caused by unknown sound speed variation, and ϵ_{traj}, caused by unknown ray trajectories. Based on Section II-B1, RAR compensated for the bias error ϵ_{ss} by replacing constant sound speed with a corrected sound speed c_{ss}. However, a considerable error ϵ_{traj}, due to refraction and reflection, persisted, as indicated by the black dotted line in the middle. Fluctuations in the dotted line occurred according to the patterns of the trajectory of the fastest rays. In other words, as the fastest rays, additional reflections of around 2,000 m, 4,000 m, and 5,000 m might have added to the trajectory error. After compensating for both displacements, RRFR and RAR showed steady and reliable performance in terms of accuracy, as shown by the solid red line and the dashed blue line at the bottom, respectively. It is noteworthy that the proposed scheme works reliably in greater measurement error (*i.e.,* adjusting σ_r up to 1.0% of actual distance d).

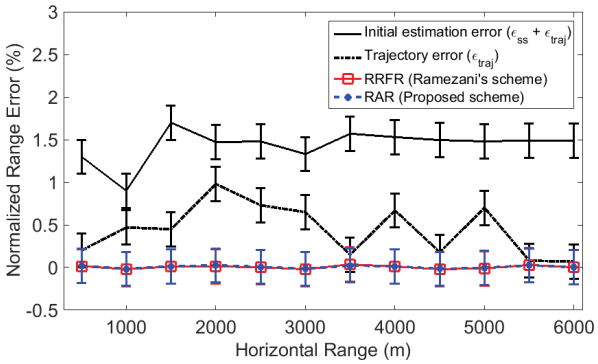

Fig. 2. Relative error as a function of range.

We also compared both schemes with respect to the average computation time (omitted in the plot due to limitations of space) to confirm that RAR provides a better tradeoff than RRFR. The average computation times of RAR for ranging were $2.15s$ and $2.38s$ for distances of 4,800 m and 5,800 m whereas those of RRFR were $16.32s$ and $18.56s$, respectively. The major portion of the computation time was approximately proportional to the number of ray tracing iterations. Since RRFR performs binary search until it finds the target distance at a given resolution, its average number of iterations is $O(log\ n)$, where n is the total size of the resolvable ranges. In our simulations, RRFR at a resolution of 0.1 m used from 12 to 15 iterations in each case. On the contrary, RAR always used only two iterations to perform two compensations (*i.e.,* at least six times shorter than that of RRFR). This significant improvement was due to its harnessing of ray pattern locality, thereby significantly reducing the number of ray tracing iterations needed to achieve a similar accuracy to RRFR. Furthermore, as the horizontal distance d between the nodes and the number of launched rays N_{ray} increased, the increase in the computational time of RRFR was quite steep. By contrast, RAR shows a moderate increment in computational time for ranging estimation.

IV. Experimental Results

In this section, we present the experimental results obtained in the ocean near Jeju Island in Korea, over an area spanning 100 km in the northern East China Sea. The logbook was called the Shallow-water Acoustic Variability EXperiment 2015 (SAVEX15) [9]. SAVEX15 was conducted to obtain environmental and acoustic data for scientific studies. As shown in Fig. 3(a), we only present two measurement cases (*i.e.,* approximately 4,800 m and 5,800 m from the source), and we evaluated the accuracies of RAR and RRFR on a real-life testbed. In these experiments, we used

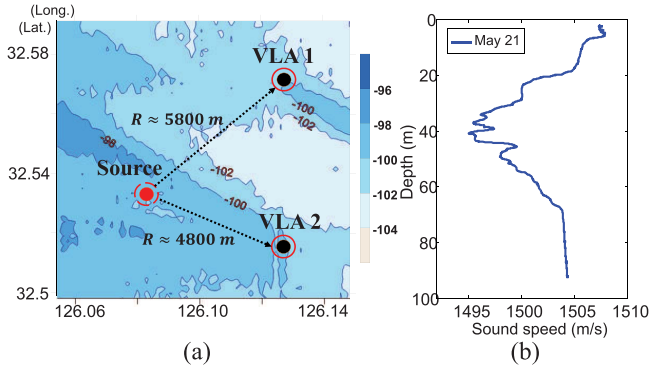

Fig. 3. System installation and measured oceanographic data near Jeju Island in [9]: (a) locations of the source and receivers with seafloor bathymetry; (b) an instance of the measured sound speed profile on May 21.

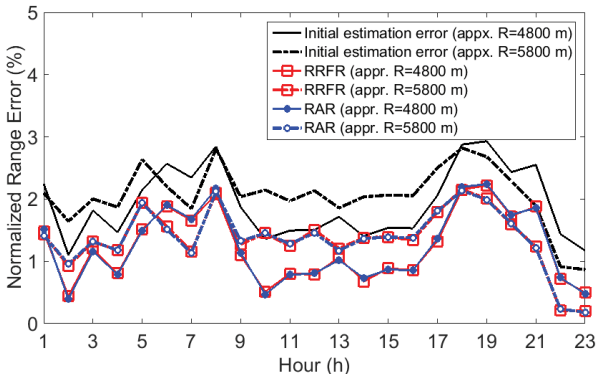

Fig. 4. Range error relative to ground truth over time.

the measured ToAs and compared RAR's estimations to the ground truth d_{gps} obtained from global positioning system (GPS) logs over a number of hours.

As shown in Fig. 3(a), the experiments were conducted in shallow water (*i.e.,* depth of approximately 100 m), and the measurements were entered into Bellhop simulations as bathymetry information. The measured SSP information shown in Fig. 3(b) was also logged over SAVEX15. To obtain the ToA measurements, we deployed a tethered source and two receivers, VLA1 and VLA2, at a depth of 40 m. The tethered source transmitted M-sequence signal with 1,023 lengths and a center frequency of 22kHz, and logged ToAs into two receivers every hour for a day. To reduce the receivers' mobility due to oceanic currents, each was attached to a heavy anchor at the bottom of the sea and equipped with an underwater buoy to provide tension against drag at a depth of 20 m. Furthermore, we compensated for the GPS position of the receivers through integrated tilt sensors. Readers may refer to SAVEX15 [9] for more detailed information.

In Fig. 4, we compare the RAR and the RRFR schemes in terms of the NRE (*i.e.,* $NRE(\%) = \frac{\hat{d}-d_{gps}}{d_{gps}} \times 100$) in the two cases. The solid blue line at the bottom and the dashed line shows the accuracies of RAR at 4,800 m and 5,800 m, respectively. The overlapping solid red line and the dashed line shows that the accuracy values of RRFR were almost identical to those of RAR, for each distance measure. Moreover, we observed that RAR and RRFR exhibited similar patterns compared to the initial estimation error (*i.e.,* the uppermost solid black line and the dotted line) with significantly improved accuracy—approximately 32 m and 40 m over time at the two cases, respectively.

In the experimental results, we observed that the NRE of RAR varied between 0.3-2.0% over a number of hours. Nevertheless, the errors were larger than in the simulation results (Section III). This gap between simulation and experiment was not simply due to the limited consideration accorded in the simulations, but was caused by multiple factors (*i.e.,* node mobility and inter-node time synchronization) [1]. Moreover, a recent experimental study in [10] has shown that ToA estimations fluctuate because of severe multipath fading and the Doppler spread that arises from nodes or the motion of water. Even worse, the direct path may not exhibit the strongest energy, which adds greater ambiguity to arrival time estimation. It is noteworthy that the effect of these slightly reduced accuracy values on real world applications can be further compensated for by refinement methods, such as Taylor-based least squares, weighted Taylor-based least squares, and constrained total least squares [11].

V. Conclusion

In ranging estimation, two main biased displacements occur due to unknown sound speed variations and acoustic ray trajectories. To compensate for these errors and reduce the computational overhead for real-time use, we here proposed RAR, a novel ranging scheme for a real-time localization system. RAR exploits ray pattern locality, and thus renders ranging estimation practical for real-time systems by significantly reducing the search space compared to state-of-the-art solution, RRFR. Our simulation and experimental studies verified that the RAR scheme can achieve better tradeoff between accuracy and computational overhead than RRFR.

References

[1] H.-P. Tan, R. Diamant, W. K. G. Seah, and M. Waldmeyer, "A survey of techniques and challenges in underwater localization," *Ocean Eng.*, vol. 38, pp. 1663–1676, Oct. 2011.

[2] M. Erol-Kantarci, H. T. Mouftah, and S. Oktug, "A survey of architectures and localization techniques for underwater acoustic sensor networks," *IEEE Commun. Surveys Tuts.*, vol. 13, no. 3, pp. 487–502, 3rd Quart., 2011.

[3] P. M. Ameer and L. Jacob, "Localization using ray tracing for underwater acoustic sensor networks," *IEEE Commun. Lett.*, vol. 14, no. 10, pp. 930–932, Oct. 2010.

[4] H. Ramezani and G. Leus, "Ranging in an underwater medium with multiple isogradient sound speed profile layers," *Sensors*, vol. 12, no. 3, pp. 2996–3017, 2012.

[5] *Ocean Acoustic Library*. Accessed on Jul. 5, 2017. [Online]. Available: http://oalib.hlsresearch.com

[6] D. Mirza, P. Naughton, C. Schurgers, and R. Kastner, "Real-time collaborative tracking for underwater networked systems," *Ad Hoc Netw.*, vol. 34, pp. 196–210, Nov. 2015.

[7] N. F. Josso, C. Ioana, J. I. Mars, and C. Gervaise, "Source motion detection, estimation, and compensation for underwater acoustics inversion by wideband ambiguity lag-Doppler filtering," *J. Acoust. Soc. Amer.*, vol. 128, no. 6, pp. 3416–3425, 2010.

[8] B. Alavi and K. Pahlavan, "Modeling of the TOA-based distance measurement error using UWB indoor radio measurements," *IEEE Commun. Lett.*, vol. 10, no. 4, pp. 275–277, Apr. 2006.

[9] H. C. Song *et al.*, "Shallow-water acoustic variability experiment 2015 (SAVEX15) trip report," Marine Phys. Lab./Scripps Inst. Oceanography, La Jolla, CA, USA, Tech. Rep., Aug. 2015.

[10] H. Huang, Y. R. Zheng, and W. Duan, "Pseudo-noise based time of arrival estimation for underwater acoustic sensor localization," in *Proc. Oceans*, 2016, pp. 1–5.

[11] J. Wan, N. Yu, R. Feng, Y. Wu, and C. Su, "Localization refinement for wireless sensor networks," *Comput. Commun.*, vol. 32, pp. 1515–1524, Aug. 2009.